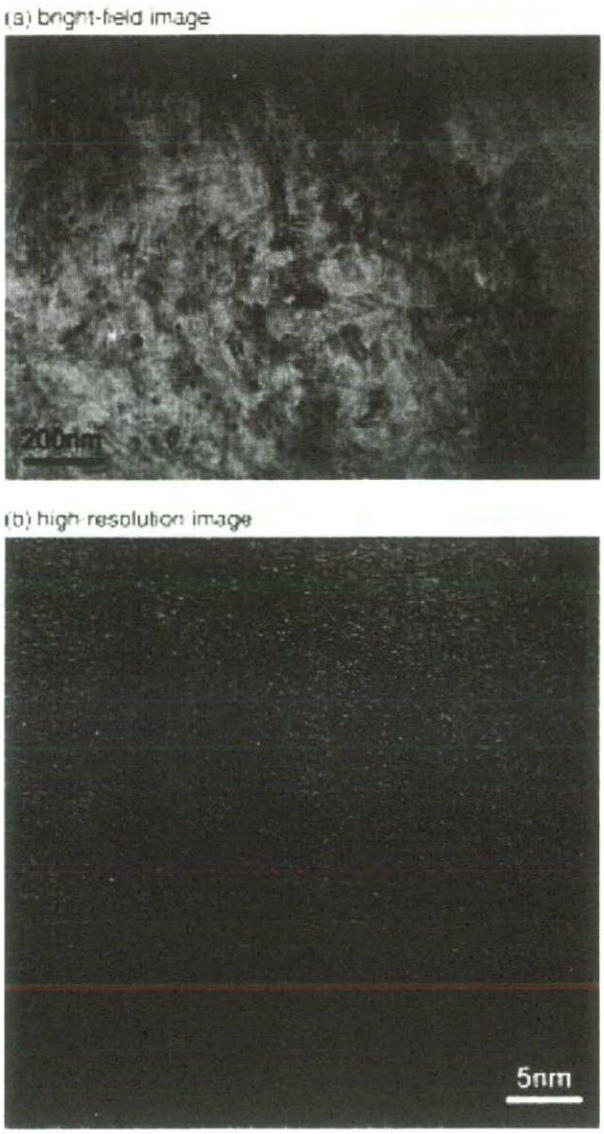

Fig. 4. (a) A bright-field image of MWCNTs implanted in the subcutaneous tissue of rat at 1 year and (b) the corresponding HRTEM images of the MWCNTs.

that indicated the disconnection of the nanotube is shown in Fig. 5. Each break of arc is indicated by white arrows. In particular, deterioration of the nanotube at the edge was remarkable. Such deterioration was seldom seen in the tissue of 1-week implantation.

Discussion

Presently observed clustering of MWCNTs which were implanted in the subcutaneous tissue indicates that the degree of the aggregation of the MWCNTs slightly decreased after the 1-year implantation. At the same time, some of separated nanotubes from the clustered MWCNTs were observed

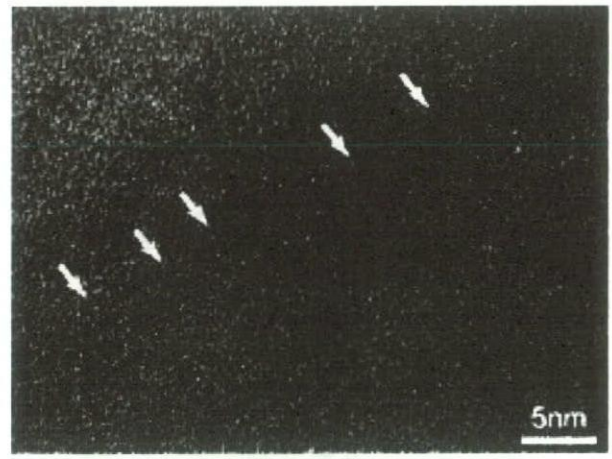

Fig. 5. HRTEM image of a MWCNT implanted in the subcutaneous tissue of rat at 1 year. The arrows indicate the deterioration sites of the graphene layers of the MWCNT.

in lysosomes after the 1-year implantation. The MWCNTs covered by the lysosomal membranes were reduced in length and appeared translucent. The same tendency has been reported by Yokoyama *et al.* on CNFs implanted in the subcutaneous tissue of rats [20] concluding that the structural changes which occurred in lysosomes and cytoplasm were attributable to the delamination of the graphene layers due to the intercalation of hydrophilic substances such as enzymes and proteins in the phagocytes. Delamination by the intercalation reactions was also reported elsewhere [22,23]. The deterioration behavior of the graphene layers in the MWCNT was first reported by Ajayan *et al.* [24]; peeling of the graphene layers that started from the edge of the MWCNT in an oxidation atmosphere was followed by thinning of the nanotube. In our HRTEM observation, the deterioration of the MWCNT was remarkable at the edge of the nanotube too as shown in Fig. 5. In both, the peeling reaction of the graphene layers commonly initiated at the edge of the nanotube. In some cases, however, structural damages of the MWCNT were observed not only at the edge but also in the outer graphene layer of the nanotube. Similar deterioration in the outer graphene layer has been observed in supercritical water [25,26]. Local hydration or hydro-oxidation, i.e. the newly formed C–H or C–OH bonding with sp^3 hybridization caught by Raman spectroscopy [26], possibly initiates the introduction of the surface damage of the MWCNT. Usually, each carbon atom on a graphene layer bonds with sp^2 hybridization in-plane and π bonding occurs between the individual graphene layers. However, once the sp^3 bonding is formed in the outer graphene layer, it causes a partial peeling of the graphene layer because an electron that contributes to the π bonding is lost. Moreover, the strain field due to the formation of three-dimensional sp^3 bonding might enhance the rehybridization from sp^2 to sp^3 between the neighboring graphene layers and peeling reaction of the outer graphene layer.

The sp^2 hybridization of carbon atoms in the graphene layer is one of the strong and stable bondings and it is not easy to break the network of in-plane σ bonding. However, it is expected that the MWCNTs used in the present study would have open edges and a lot of defect sites in the outer graphene layers because the MWCNTs were exposed in the several acid/alkali solutions such as HCL, NaOH and H_2SO_4–HNO_3 during the purification process. In fact, the MWCNTs after the purification showed the hydrophilic behavior. This provides that the sp^3 hybridization due to the bonding between C–H and C–OH occurred at the outer graphene layers of the MWCNTs used in the present study. Therefore, it is considered that the peeling reaction based on the interaction between the hydrophilic substances and the carbon atoms in the outer graphene layer of MWCNTs occurs with a time passage, even though the nanotubes are put into a comparatively weak oxidation environment like *in vivo*. Observed shortening in the length of the nanotubes could occur subsequently.

Concluding remarks

We performed TEM observations on the morphology and crystallography of MWCNTs implanted in the subcutaneous tissue of rats. HRTEM was used to investigate the detailed atomic structure of the MWCNTs in the tissue. Clusters of the MWCNTs implanted in the subcutaneous tissue were well recognized by the TEM observations. It was indicated that the degree of the aggregation of the MWCNT clusters slightly decreased and some nanotubes were taken in phagocytes. The deterioration of crystalline structure of the nanotubes in phagocytes was emphasized by the HRTEM observation. It was suggested that the deterioration of the nanotubes was due to the peeling of the outer graphene layers in the phagocytes.

Acknowledgements

The authors gratefully thank Professor M. Uo and Dr T. Akasaka for their insights. The authors also acknowledge Mr K. Sugawara for his technical support in the HVTEM observations. This work is supported by Health and Labor Sciences Research Grants in Research on Advanced Medical Technology in Nanomedicine Area from the Ministry of Health, Labor and Welfare of Japan.

References

1 Pantarotto D, Partidos C D, Hoebeke J, Brown F, Kramer E, Briand J P, Muller S, Prato M, and Bianco A (2003) Immunization with peptide-functionalized carbon nanotubes enhances virus-specific neutralizing antibody responses. *Chem. Biol.* **10**: 961–966.

2 Muller J, Huaux F, Moreau N, Misson P, Heilier J F, Delos M, Arras M, Fonseca A, Nagy J B, and Lison D (2005) Respiratory toxicity of multi-wall carbon nanotubes. *Toxicol. Appl. Pharmacol.* **207**: 221–231.

3 Wick P, Manser P, Limbach L K, Dettlaff-Weglikowska U, Krumeich F, Roth S, Stark W J, and Bruinink A (2007) The degree and kind of agglomeration affect carbon nanotube cytotoxicity. *Toxicol. Lett.* **168**: 121–131.

4 Balani K, Anderson R, Laha T, Andara M, Tercero J, Crumpler E, and Agarwal A (2007) *Biomaterials* **28**: 618–624.

5 Raja P M V, Connolley J, Ganesan G P, Ci L, Ajayan P M, Nalamasu O, and Thompson D M (2007) Impact of carbon nanotube exposure, dosage and aggregation on smooth muscle cells. *Toxicol. Lett.* **169**: 51–63.

6 Balani K, Chen Y, Harimkar S P, Dahotre N P, and Agarwal A (2007) Tribological behavior of plasma-sprayed carbon nanotube-reinforced hydroxyapatite coating in physiological solution. *Acta Biomaterialia* **3**: 944–951.

7 Price R L, Waid M C, Haberstroh K M, and Webster T J (2003) Selective bone cell adhesion on formulations containing carbon nanofibers. *Biomaterials* **24**: 1877–1887.

8 McKenzie J L, Waid M C, Shi R, and Webster T J (2004) Decreased functions of astrocytes on carbon nanofiber materials. *Biomaterials* **25**: 1309–1317.

9 Jensen A W, Wilson S R, and Schuster D I (1996) Biological applications of fullerenes. *Bioorg. Med. Chem.* **4**: 767–779.

10 Lin J C and Wu C H (1999) Surface characterization and platelet adhesion studies on polyurethane surface immobilized with C_{60}. *Biomaterials* **20**: 1613–1620.

11 Gonzalez K A, Wilson L J, Wu W, and Nancollas G H (2002) Synthesis and *in vitro* characterization of a tissue-selective fullerene: vectoring $C_{60}(OH)_{16}$ AMBP to mineralized bone. *Bioorg. Med. Chem.* **10**: 1991–1997.

12 Prylutska S V, Matyshevska O P, Golub A A, Prylutskyy Y I, Potebnya G P, Ritter U, and Scharff P (2007) Study of C_{60} fullerenes and C_{60}-containing composites cytotoxicity *in vitro*. *Mater. Sci. Eng. C* **27**: 1121–1124.

13 Roberts J E, Wielgus A R, Boyes W K, Andley U, and Chignell C F (2008) Phototoxicity and cytotoxicity of fullerol in human lens epithelial cells. *Toxicol. Appl. Pharmacol.* **228**: 49–58.

14 Spesia M B, Milanesio M E, and Durantini E N (2008) Synthesis, properties and photodynamic inactivation of *Escherichia coli* by novel cationic fullerene C_{60} derivatives. *Eur. J. Med. Chem.* **43**: 853–861.

15 Bianco A, Kostarelos K, and Prato M (2005) Applications of carbon nanotubes in drug delivery. *Curr. Opin. Chem. Biol.* **9**: 674–679.

16 Smart S K, Cassady A I, Lu G Q, and Martin D J (2006) The biocompatibility of carbon nanotubes. *Carbon* **44**: 1034–1047.

17 Pulskamp K, Diabate S, and Krug H F (2007) Carbon nanotubes show no sign of acute toxicity but induce intracellular reactive oxygen species in dependence on contaminants. *Toxicol. Lett.* **168**: 58–74.

18 Pulskamp K, Worle-Knirsch J M, Hennrich F, Kern K, and Krug H F (2007) Human lung epithelial cells show biphasic oxidative burst after single-walled carbon nanotube contact. *Carbon* **45**: 2241–2249.

19 Fugetsu B, Satoh S, Iles A, Tanaka K, Nishia N, and Watari F (2004) Encapsulation of multi-walled carbon nanotubes (MWCNTs) in Ba^{2+}-alginate to form coated micro-beads and their application to the pre-concentration/elimination of dibenzo-*p*-dioxin, dibenzofuran, and biphenyl from contaminated water. *Analyst* **129**: 565–566.

20 Yokoyama A, Sato Y, Nodasaka Y, Yamamoto S, Kawasaki T, Shindoh M, Kohgo T, Akasaka T, Uo M, Watari F, and Tohji K (2005) Biological behavior of hat-stacked carbon nanofibers in the subcutaneous tissue in rats. *Nano Lett.* **5**: 157–161.

21 Sato Y, Yokoyama A, Shibata K, Akimoto Y, Ogino S, Nodasaka Y, Kohgo T, Tamura K, Akasaka T, Uo M, Motomiya K, Jeyadevan B, Ishiguro M, Hatakeyama R, Watari F, and Tohji K (2005) Influence of length on cytotoxicity of multi-walled carbon nanotubes against human acute monocytic leukemia cell line THP-1 *in vitro* and subcutaneous tissue of rats *in vivo*. *Mol. BioSyst.* **1**: 176–182.

22 Liu Z, Ooi K, Kanoh H, Tang W, and Tomida T (2000) Swelling and delamination behaviors of birnessite-type manganese oxide by intercalation of tetraalkylammonium ions. *Langmuir* **16**: 4154–4164.

23 Toomey R, Freidank D, and Ruhe J (2004) Swelling behavior of thin, surface-attached polymer networks. *Macromolecules* **37**: 882–887.

24 Ajayan P M, Ebbesen T W, Ichihashi T, Iijima S, Tanigaki K, and Hiura H (1993) Opening carbon nanotubes with oxygen and implications for filling. *Nature* **362**: 522–525.

25 Chang J-Y, Ghule A, Chang J-J, Tzing S-H, and Ling Y-C (2002) Opening and thinning of multiwall carbon nanotubes in supercritical water. *Chem. Phys. Lett.* **363**: 583–590.

26 Park K C, Hayashi T, Tomiyasu H, Endo M, and Dresselhaus M S (2005) Progressive and invasive fictionalization of carbon nanotube sidewalls by diluted nitric acid under supercritical conditions. *J. Mater. Chem.* **15**: 407–411.

単細胞個体・ゾウリムシのカーボンナノチューブ細胞内摂取のリアルタイム観察

芳賀信幸*

JJSB

Real-time observation of carbon nanotubes uptake in unicellular organism, Paramecium

The establishment of a standard method for the judgment of cytotoxicity of nanoparticles is one of the important problems to be quickly developed. We consider *Paramecium*, a unicellular eukaryotic organism, as a model system for the cytotoxicity test of nanoparticles because of their multiple cellular functions. By the observation of real-time uptake in *Paramecia*, it has been revealed that multiple-walled carbon nanotubes (MWCNT) have no remarkable cytotoxicity but high biocompatibility. Furthermore, MWCNT increased in growth rate when added in culture medium. The understanding of the mechanism of MWCNT effect on growth rate would be an important subject in near future.

ナノ微粒子に対する細胞毒性評価法の確立は緊急課題の一つである．単細胞性真核生物であるゾウリムシは多機能同時発現細胞として細胞毒性試験に適した実験生物である．細胞内取り込みリアルタイム観察により，多層カーボンナノチューブはゾウリムシに対して細胞毒性は示さず，高い親和性を持つことが明らかになった．さらに，多層カーボンナノチューブを培養液に添加することによって，細胞増殖速度が上昇することが明らかになった．

多層カーボンナノチューブのバイオ応用を視野に入れた増殖効果に関する分子機構の解明が，今後の重要な課題となるだろう．

*Nobuyuki Haga**

Key words：多層カーボンナノチューブ，細胞内取り込み，細胞増殖，ゾウリムシ（*Paramecium caudatum*）

ゾウリムシの細胞特性と生態的ニッチ

ゾウリムシ（*Paramecium caudatum*）は，原生生物繊毛虫類に属する単細胞生物で，中学や高校の教材にも用いられるなど，原生生物のなかでは最もよく知られている生物の一つである[1]．細胞は長軸約200 μm，短軸約20～30 μmの回転楕円体をしており，細胞の表面は規則的な配列パターンを持つ約10 μmほどの繊毛によって覆われている（図1）．世界中の淡水域（池，沼，湖，下水道など）から採集され，細胞学，遺伝学，電気生理学など生物学の幅広い分野で研究対象とされている．

系統分類学的には，ゾウリムシは真核生物に分類され，細胞の内部構造や遺伝情報の基盤となる複製・転写・翻訳系はヒトをはじめとする多細胞生物と共通である．また，大腸菌などの細菌類を餌とし，ミジンコなどの小型節足動物やメダカなどの小型魚類および稚魚などの餌となるため，生態学的にも重要なニッチ（生態的地位）を占めている[2～4]．

ゾウリムシの生活史は，接合からはじまる．接合は，多細胞生物の受精に相当する現象である．多細胞生物では，親となる個体から卵と精子がつくられ，受精後に新しい世代が生まれる．一方，ゾウリムシでは，親となる細胞から配偶核がつくられ，接合の間に両方の親細胞からつくられた配偶核同士で核融合が起こり，新しい世代の基盤となる核が出来上がる．この核を引き継いだ細胞が，新しい世代としてライフサイクルをはじめる[5]．

接合は交配実験の手段として，古くから利用されてきた[6]．世界のどの地域で採集されたゾウリムシでも，交配実験を行い，新しい子孫をつくることが出来れば同じ種として判定され，登録されることになる．現在では，種に相当する16のグループ（syngen）

* Department of Biological Technology, Senshu University of Ishinomaki
石巻専修大学理工学部生物生産工学科
［略歴］　1974年 東北大学理学生物学科卒業．1979年 東北大学大学院理学研究科博士課程修了（理学博士）．1980年 ウィスコンシン大学分子生物学研究所研究員．1989年 石巻専修大学助教授．1997年 同教授，現在に至る．専門：細胞生物学，細胞工学，クローナルエイジングの分子機構に関する研究．趣味：テニス，リコーダー

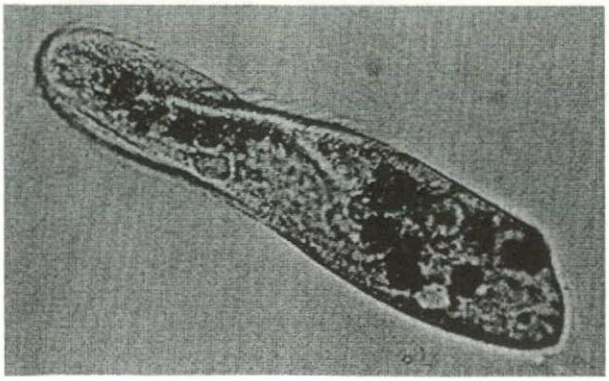

図1　Fe_2O_3を取り込んだゾウリムシ(生細胞)
細胞の表面には波打っている繊毛が見える.

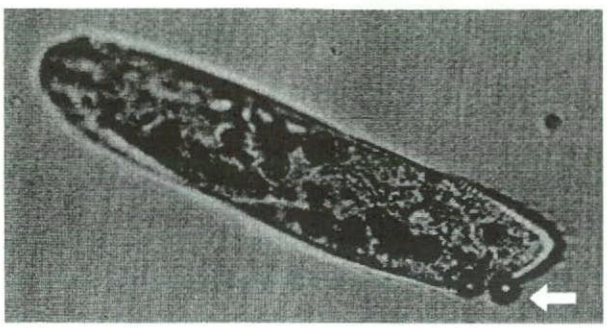

図2　TiO_2を取り込んだゾウリムシ(生細胞)
未消化のTiO_2を含む食胞が細胞肛門から放出された瞬間(矢印)

が記載されている.

ゾウリムシは実験室では通常25℃付近で培養するが，培養条件がよければ約8時間に一度の割合で細胞分裂を行う．このとき，ゾウリムシは細胞の表面に形づくられている細胞口から培養液中のバクテリアや固形物，液体成分などを取り込み，細胞質内に食胞とよばれる特殊な球状の小胞を形成する．食胞は，ライソゾームなどの消化系小胞と融合しながら細胞内を移動し，取り込んだ成分を消化・吸収する[7]．その後，消化できなかった成分は細胞肛門から順次排泄される(図2)．

ゾウリムシには，温度，pH，各種陽イオンなどに応答する多彩な機能が備わっている．通常これらの機能は環境要因の変動に応じて発現し，遊泳行動として把握することが出来るので，ゾウリムシは“動く感覚細胞”や“動く神経細胞”とよばれる[5]．また，細胞分裂能力も高く，安定している．1個の細胞から培養を開始することが出来るので，細胞分裂に対するさまざまな物質の影響を定量的に比較解析

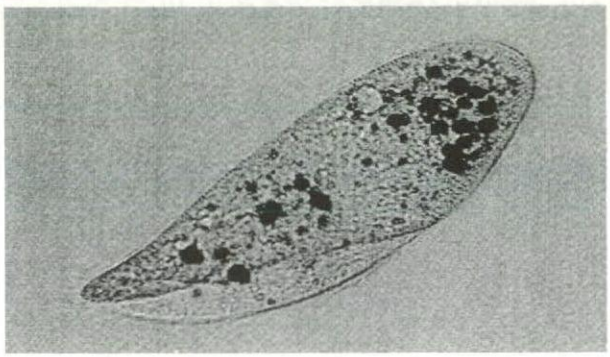

図3　生理食塩水中でのMWCNTの取り込み
黒い球状の食胞にはMWCNTが濃縮されて取り込まれている.

表1　MWCNTを含む生理食塩水中でのMWCNTの初期取り込み速度

時間(分)	食胞数/細胞			
	平均	標準偏差	n	ANOVA(Tukey)
1	0	0	10	a
2	0	0	10	a
3	0.7	0.9	10	a
4	1.1	0.9	10	b

多重比較による統計検定(ANOVA, Tukey)の結果は，異符合間でP＜0.01で有意であることを示している．nは個体数

することが可能である.

以上のように，ゾウリムシはナノ微粒子の生体組織に対する為害性やバイオ応用への可能性を検討するうえで，すぐれたバイオアッセイ系を提供するものと考えられるが，基礎的な研究の報告例はきわめて少ない．本稿では，ゾウリムシの食胞形成を指標として，多層カーボンナノチューブ(multi-walled carbon nanotubes : MWCNT)の細胞内摂取とその後の動態について，オリジナルデータをもとに解説する．また，MWCNTの細胞分裂に対する影響についても新しい知見に基づいて考察する.

生理食塩水中でのMWCNTの取り込みと細胞内動態

金沢で採集されたゾウリムシ(KNZ0501)を用いて，生理食塩水(K-DS : NaをKに置き換えたDryl氏液)に分散した多層カーボンナノチューブ(MWCNT A1，50 ng/μL，NanoLab社)の細胞内取り込み速度を測定した(図3)．取り込み速度は形成された食胞の数を指標として算出したが，後述する

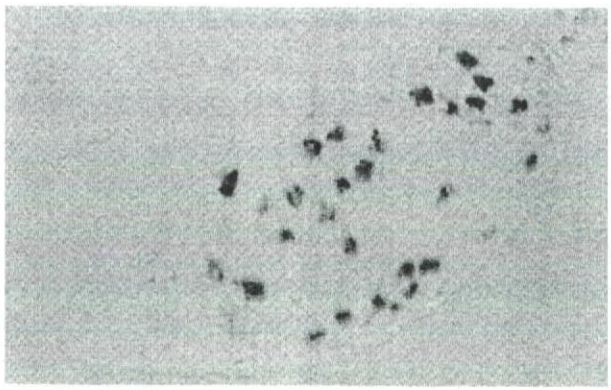

図4　MWCNTを含む生理食塩水中でのMWCNTの取り込み（25分後）

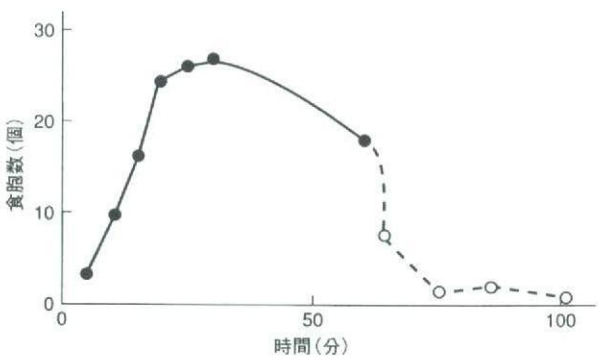

図5　MWCNTを含む生理食塩水中でのMWCNTの取り込みおよび細胞内滞在時間
黒マルはMWCNTを含む生理食塩水中でのMWCNTの取り込みをあらわす．また，白マルはMWCNTを含まない生理食塩水に細胞を移したあとでの食胞数をあらわす．

ように食胞内のMWCNT量は時間とともに変化するため，必ずしもMWCNTの絶対量を反映したものではない．

初期の取り込み特性を示した（表1）．MWCNT分散液100 μLにゾウリムシを入れ，25℃でインキュベートし，一定の時間ごとに細胞を取り出して顕微鏡下で食胞数をカウントした．ゾウリムシははじめの2分間はMWCNTをまったく取り込まなかった．3分後から少量ずつMWCNTを取り込みはじめ，色の薄い食胞が形成されるようになり，4分後にはMWCNTを多量に含んで黒くなった食胞が認められるようになった．

その後，時間の経過とともにMWCNTを取り込んだ食胞形成が活発になり，図4に示すように，一定のサイズの食胞が細胞全体に分布するようになった．取り込み開始5分後から細胞内食胞数がピークに達

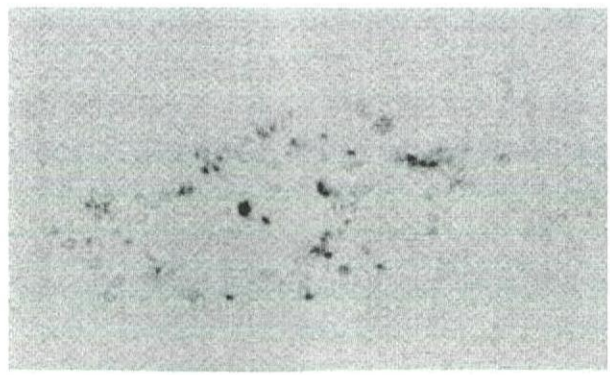

図6　生理食塩水中でのMWCNTの取り込み（取り込み終了から60分後）

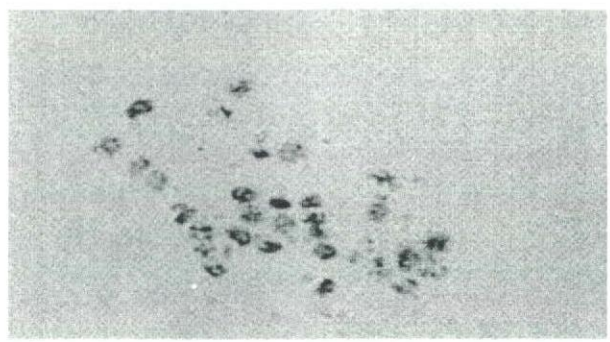

図7　MWCNTを含む生理食塩水中でのMWCNTの再取り込み（40分後）

表2　MWCNTを含む生理食塩水中でのMWCNT取り込み終了後の細胞内滞在時間

時間（分）	食胞数/細胞			
	平均	標準偏差	n	ANOVA（Tukey）
再取り込み後				
20	17.6	3.5	10	a
60	22.4	5.4	10	b
取り込み終了後				
25	13.7	5.4	10	a

多重比較による統計検定（ANOVA, Tukey）の結果は，異符合間で$P < 0.01$で有意であることを示している．nは個体数

するまでの間の平均食胞形成速度は約1食胞/分であった（図5）．

つぎに，MWCNTを取り込んだ食胞の動態を調べるために，60分間MWCNT分散液中でインキュベートした細胞を生理食塩水に移し，さらに60分間，顕微鏡下で食胞の変化を観察した．すると，図6に示すように，食胞の数は減少し，個々の食胞内のMWCNT量も低下していることが明らかになった．

別の実験から，ゾウリムシは長時間MWCNT分散液中にインキュベートしておくと，しだいに

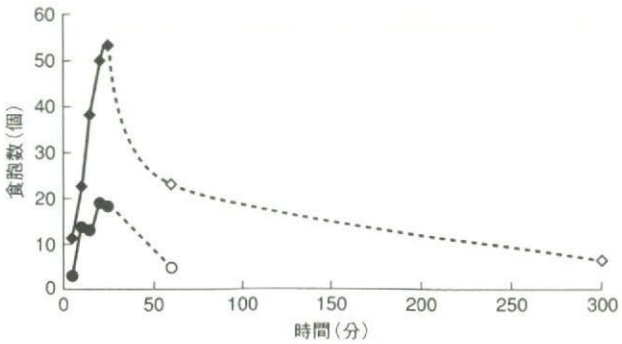

図8　培養液および生理食塩水中でのMWCNTの取り込みと細胞内滞在時間

黒ダイヤモンドは培養液中でのMWCNTの取り込み，黒マルは生理食塩水中でのMWCNTの取り込みをあらわす．また，白ダイヤモンドと白マルはそれぞれMWCNTを含まない生理食塩水に細胞を移したあとでの食胞数をあらわす．

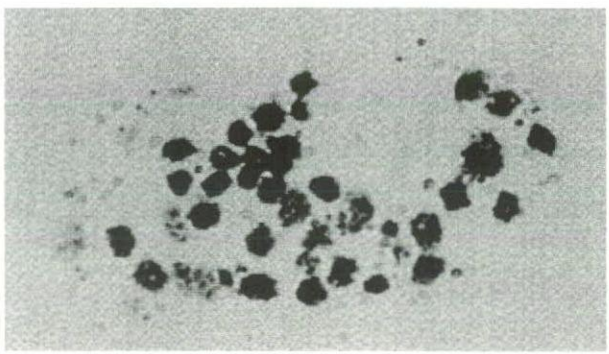

図9　培養液中でのMWCNTの取り込み（10分後）

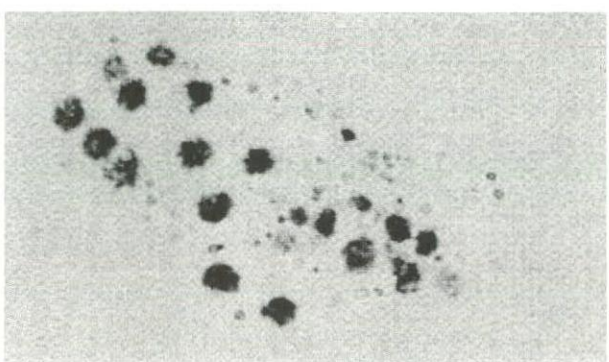

図10　培養液中でのMWCNTの取り込み（取り込み終了から60分後）

MWCNTを取り込まなくなり，約50分後には細胞内からMWCNTを含む食胞はほとんど消失してしまうことがわかった．このような細胞を新しいMWCNT分散液に移すと，再びMWCNTを活発に取り込みはじめ，図7に示すように約40分後には最大時のレベルまで達することが明らかになった．

表3　MWCNTの細胞増殖に及ぼす影響（初期分裂速度）

	細胞数/24時間			
	平均	標準偏差	n	ANOVA（Tukey）
生理食塩水＋MWCNT	1	0	12	a
培養液＋MWCNT	4	0	12	b
生理食塩水	1	0	12	a
培養液	2.1	0.3	12	c

多重比較による統計検定（ANOVA, Tukey）の結果は，異符合間でP＜0.01で有意であることを示している．nは個体数

表4　MWCNTの細胞増殖に及ぼす影響（継続培養）

	樹立クローン（%）	n
生理食塩水＋MWCNT	100	12
培養液＋MWCNT	100	12
生理食塩水	100	12
培養液	100	12

nは個体数

食胞に取り込まれたMWCNTの細胞内滞在動態に関する特性を示した（表2）．また，図5には取り込み開始の初期過程から排泄完了までの時間経過を示した．これらの図表から，ゾウリムシはMWCNTを好んで取り込むが，数十分後からは取り込みを停止する性質を持っていることが示唆される．なお，実験期間中，MWCNTの細胞毒性を示唆するような現象はまったく認められなかった．

培養液中でのMWCNTの取り込み

MWCNT単独での細胞内取り込み特性および滞在動態が明らかになったので，つぎに，培養液中でのMWCNTの取り込みについて検討した．培養液は本研究室で常用しているもので，1.5%レタスジュースを含むK-DS溶液にバクテリア（*Klebsiella pneumoniae*）を接種し，25℃で24時間インキュベートしたものを用いた（MWCNT，50 ng/μL，100 μL）[8]．

図8および図9に示すように，MWCNTを含む食胞は生理食塩水の場合よりも速い速度で形成されており，図8から求められた平均食胞形成速度は2.2食胞/分であった．また，細胞内滞在時間も生理食塩水の場合よりはるかに長く，取り込み開始後300分でも，すべての細胞でMWCNT食胞の存在が認められた（図10）．

培養液中でのMWCNTには食胞形成を促進する

効果があることがわかったので，つぎに，細胞増殖に対する影響について検討した．50 ng/μL のMWCNT を含む実験群と対象群を比較した結果，表3に示すように，MWCNTはインキュベーション開始からはじめの24時間における細胞分裂速度を，MWCNTを含まない培養液にくらべて約2倍促進することが明らかになった．

また，1細胞から開始した継続培養の結果を表4に示した．これは，48時間 MWCNT を含む溶液中でインキュベートしたあと，MWCNTを含まない培養液に移し，1週間の継続培養を行ったものである．いずれの実験群においてもすべての細胞が細胞分裂を行い，それぞれクローンを樹立したことを示している．

まとめと展望

今回使用したNanoLab社製MWCNT(番号1)は溶液中での分散性が低いため，使用前に，あらかじめメノウ乳鉢で細かくすり潰した．また，MWCNTを溶かした溶液は，使用前に20分間の超音波処理を施したあと，ボルテックスで約1分間撹拌した．しかしながら，MWCNTの凝集塊形成を防ぐことは出来なかった．今後，ゾウリムシに対する実質的な有効分散量を特定するためには，分散性の高い溶液の調整法を検討し，開発する必要がある．

本実験は，MWCNTの細胞毒性の発現を見逃すことがないように，充分な配慮のもとに実験条件を設定した．しかし，MWCNT の細胞毒性に関しては，特筆すべき重大な所見はまったく認められなかった．

一方，MWCNTはゾウリムシに対して食胞形成促進作用と長時間の細胞内滞在性を示した．さらに，この知見は MWCNT を培養液中に添加することによる細胞増殖促進効果として裏付けられた．この増殖促進効果は予想外の成果であり，今後，分子機構の解明や多細胞生物由来の培養細胞系に対する効果の検討結果によっては，医療や健康促進などの分野で大いに活用できる可能性がある．

文　献

1) 樋渡宏一：ゾウリムシの性と遺伝．東京大学出版会，東京，1982.
2) Porter KG, Pace ML, Battey JF : Ciliate protozoans as links in freshwater planktonic food chains. Nature 1979, 277 : 563-565.
3) Tezuka Y : An experimental study on the food chain among bacteria, *Paramecium* and *daphnia*. Int Rev Gesamten Hydrobiol 1974, 59 : 31-37.
4) Eaton RC, Farely RD : Growth and the reduction of depensation of zebra-fish, *Brachydanio rerio*, reared in the laboratory. Copeia 1974, 1 : 204-209.
5) 樋渡宏一・編：ゾウリムシの遺伝学．東北大学出版会，仙台，1999.
6) 樋渡宏一，月井雄二：微生物遺伝学実験法．(石川辰夫・編)，共立出版，東京，1982, p302.
7) Fok AK, Paeste RM : Lysosomal enzymes of *Paramecium caudatum* and *Paramecium tetraurelia*. Exp Cell Res 1982, 139 : 159-169.
8) Hiwatashi K : Determination and inheritance of mating type in *Paramecium caudatum*. Genetics 1968, 58 : 373-386.

Original

Paramecium as a bioassay system for elucidation of cytotoxicity and biocompatibility of nanoparticles: effects of carbon nanofibers on proliferation and survival

Nobuyuki HAGA[1]* and Koichi HANEDA[2]

[1]*Department of Biological Technology,* [2]*Department of Information Technology and Electronics, Senshu University of Ishinomaki, Ishinomaki, Miyagi 986-8580, Japan*

SUMMARY

Carbon nanofibers (CNF), composed of carbon nanotubes, are a recent technological advance with wide applications in nano-engineering fields including biotechnology and biomedicine. However, little is known about the environmental effects of CNF, or their potential danger to human health. To elucidate the safety of CNF, we examined the cytotoxicity of CNF in *Paramecium*. In this study we considered the cytotoxicity effect of CNF in two categories of cellular properties, cell survival and cell proliferation. We show that CNF are ingested and concentrated as efficiently as nutritive bacteria by paramecia, revealing a means by which CNF could be introduced into the food webs of aquatic ecosystems. Clear cytotoxicity of CNF was detected in survival tests by extracellular application at extremely high concentration (up to 50 mg/ml) in culture medium containing nutritive bacteria. Contrary to this effect, no cytotoxicity was detected in survival tests using the modified Dryl's solution (K-DS) that is used as a buffered saline of culture medium. The cytotoxicity of CNF suggests an interaction between CNF and the components in culture medium or their metabolic products produced by digestion of components in culture medium. Another cytotoxicity effect was detected in proliferative activity test at lower concentrations of CNF (up to 500 μg/ml). The cytotoxicity on proliferative activity was reversible and recovery occurred within 24 hours after removal of CNF. Our results suggest that *Paramecium* is useful for a bioassay of nanoparticle cytotoxicity. For the elucidation of safety of CNF we have to examine both the optimum concentration of CNF and co-existing biomaterials in a test solution. In conclusion, CNF have a high potential for cytological and biomedical application under precise control of concentration.

*Corresponding author
Tel: +81-225-22-7716, Fax: +81-225-22-7746
E-mail: haga@isenshu-u.ac.jp
Received:5 March 2006; Accepted:10 September 2007

INTRODUCTION

The safety of materials to living organisms usually depends upon particle size: substances that are safe in macroscopic quantities can become dangerous when reduced to microscopic particles (Brown et al, 2001). As the behavior of nanoparticles in the environment and in cells is not well understood, it is important to establish an experimental system in which to assess the effects of nanoparticles on the environment and on living organisms.

Paramecium, a ciliated eukaryotic unicellular organism that lives in fresh water, has several features that make it a potentially valuable model to assay the cytotoxicity of environmental agents (Rajini et al, 1989, Smith-Sonneborn et al, 1983, 1986): they can ingest both soluble molecules and many different types of particle, including polyethylene particles, India ink, iron filings and sand, by phagocytosis, and they show very stable cellular functions such as phagocytosis, cell division and swimming behavior. In this study, we examine the use of *Paramecium* as a bioassay for evaluating the cytotoxicity of nanoparticles and have established a standard experimental method that enables micro liter-sized assays.

The CNF used in this experiment have a structure of hollow graphitic tubules of nanometer dimensions, and are comprised of coaxial tubes of helically arranged carbon-hexagon sheets. Typically, their diameters ranged from 2 to 20 nm, and they were several micrometers in length (Iijima, 1991).

MATERIALS AND METHODS

Cells and culture medium

Paramecium caudatum, syngen 3 was used in this study. They were grown at 25°C in a culture medium containing 1.25% (w/v) fresh lettuce juice diluted with K-DS (Dryl's solution (Dryl, 1959) modified by substituting KH_2PO_4 for NaH_2PO_4, pH 7.0 (Yanagi, 1987)) and inoculated with *Klebsiella pneumoniae* one day before use (Hiwatashi, 1968).

CNF production

CNF were provided by Prof. K. Tohji (Tohoku University, Japan). They were produced in a conventional flow reactor system (Rodriguez, 1993) in which a hydrocarbon/carrier-gas mixture (C_2H_4/H_2 (4:2)) was pyrolysed at 873 K for 4 hours in the presence of powdered Ni catalyst. The catalyst was positioned in an Al_2O_3 boat and set in a quartz tube assembled in a horizontal tube furnace; it had been reduced in advance in a 10% H_2/He stream for 2 hours at 873 K.

As the CNF inevitably contain an appreciable amount of metallic elements, such as Ni, a purification process is vital to both fundamental studies and potential applications of the material (Ebbesen et al, 1994; Tohji, 1996). The CNF used in this study were purified by hydrochloric acid treatment (Tohji et al, 1996).

CNF ingestion

CNF were washed twice with K-DS with centrifugation at 10,000 rpm for 5 min. The washed CNF were suspended at a concentration of 100 mg/ml in K-DS. Paramecia were washed twice with K-DS by a hand centrifuge and suspended in K-DS at the cell density of about 4,000 cells/ml. Then, 40 µl of the CNF suspension was mixed with an equal volume of the cell suspension and the mixture was incubated at 25°C. The paramecia were periodically isolated from the mixture with a hand-made glass micropipette and put into a drop of 2.5%(w/v) methyl cellulose dissolved in K-DS on a glass slide. Photographs were taken under a light microscope (ZEISS AX10) by a digital camera (Nikon, DS-5Mc).

Cytotoxicity test of CNF

A CNF suspension was prepared in an autoclaved glass depression slide with an autoclaved microchip by mixing CNF stock suspension with either K-DS or fresh culture medium. Then, a single paramecium was added into 100 μl of the CNF mixture with a hand-made glass micropipette under a binocular microscope. The CNF suspension with the paramecium was incubated at 25°C.

Capillary culture method

We developed a small-sized bioassay using a glass capillary (0.6 mm inside diameter and 35 mm length) by modification of the method (Haga and Hiwatashi, 1981). Twenty μl of a CNF suspension containing paramecia was put on a glass depression slide and then the suspension was drawn into a capillary by capillary action. The capillary was placed in a laboratory dish with a sheet of wet paper. This method allows a one-week incubation at 25°C without any serious problem of evaporation of the medium.

Statistic analysis

Statistical analysis of the data from the dose-effect experiments was performed using the Dunnett test (Graph pad Prism 4).

RESULTS

Ingestion of CNF and food vacuole formation

Paramecia ingest nutritive bacteria via the buccal cavity and concentrate the bacteria, together with a small amount of fluid, in food vacuoles. CNF-containing food vacuoles are shown in Figure 1a and 1b. Immediately after initial contact with CNF Paramecia began to ingest CNF by forming a food vacuole. CNF particles were concentrated in each food vacuole. No CNF particle that escaped from a food vacuole into cytoplasm was detected by a light microscope observation.

Effect of CNF on non-proliferating cell survival

Before testing the cytotoxicity of CNF, we examined experimental conditions to prepare homogeneous dispersion of CNF suspension in K-DS. By varying the concentrations of CNF and the time of sonication, we confirmed that a homogeneous suspension of CNF could be obtained in up to a concentration of 50 μg/ml in K-DS for 20 min sonication.

Paramecia do not undergo proliferation when incubated in a bacteria-free solution. The survival of non-proliferating paramecia was examined by using a capillary culture with 20 μl of CNF suspension in K-DS. In the presence of 50 mg/ml of CNF, all of the tested cells remained alive through-

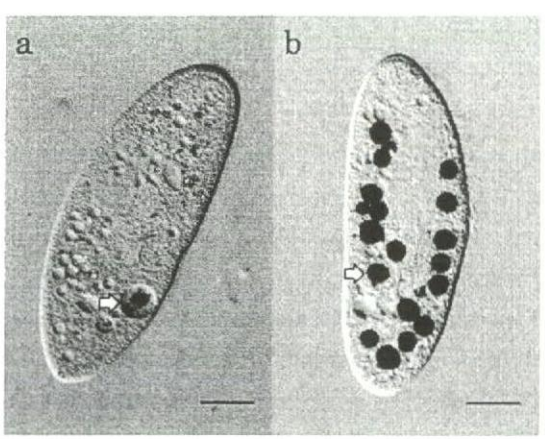

Fig. 1. A photograph of a living *Paramecium* ingesting CNF. a: At 1 min after the initiation of incubation in a CNF suspension (50 mg/ml), a cell was isolated in 2.5% (w/v) methyl cellulose dissolved in K-DS and mounted on a glass slide. Then, about 5 min later, a photograph was taken with a digital camera (Nikon, DS-5Mc) attached to a light microscope (ZEISS AX10). A white arrow shows aggregating CNF particles in a food vacuole. b: A photograph was taken at 20 min after the initiation of incubation in the CNF suspension. Black particles, one of which is shown by a white arrow, indicate CNF-containing food vacuoles. Bar is 30 μm.

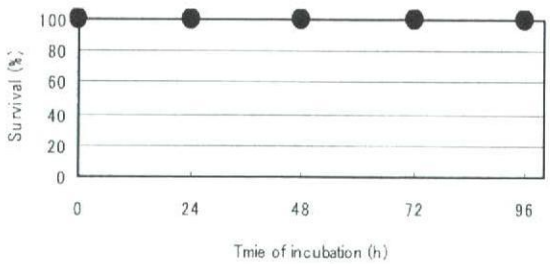

Fig. 2a. Survival rates of non-proliferating paramecia in a 50 mg/ml CNF suspension. The abscissa shows length of time of incubation in the CNF suspension, and the ordinate shows the mean percentage of cells surviving up to 96 h after the initiation of incubation (n=6).

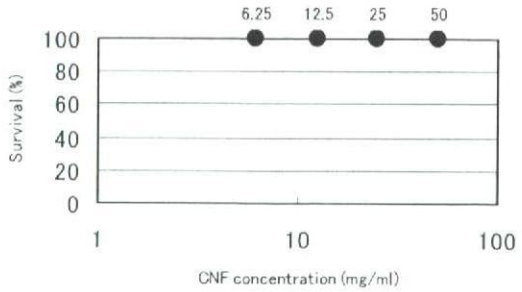

Fig. 2b. Effect of different doses of CNF on survival of non-proliferating paramecia. The abscissa shows the amount of CNF suspended in K-DS. Scale of abscissa was shown by logarithm. The ordinate shows the mean percentage of cells surviving up to 96 h after the initiation of incu-

out the period of 96 hours incubation, without any noticeable detrimental response to CNF exposure (Fig. 2a). No cytotoxicity was detected over a range of CNF concentrations up to 50 mg/ml in non-proliferating paramecia (Fig. 2b).

Effect of CNF on proliferation

The effect of CNF on the proliferation of paramecia was tested in fresh culture medium containing nutritive bacteria in a glass depression slide culture. A single cell was suspended in 200 µl of the CNF suspension (50 mg/ml) and then was kept at 25℃. Under these conditions, during the first 24 hours the paramecia underwent cell division once, but their daughter cells gradually lost the ability to swim and, after 48 hours of incubation, more than 95% died. On the other hand, cells in the control culture continued cell divisions during 48 hours of incubation (Fig. 3a).

We examined cytotoxicity effect of CNF at

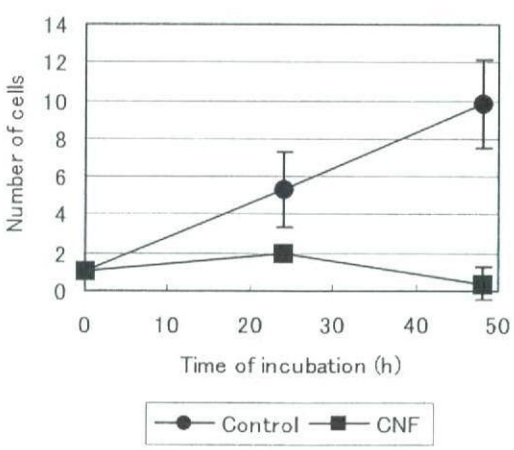

Fig. 3a. Survival of proliferating paramecia cultured in a CNF suspension. The abscissa shows time after the initiation of incubation and the ordinate shows the mean number of surviving cells in fresh culture medium containing nutritive bacteria and 50 mg/ml CNF (n=6). Control means the culture containing 0 mg/ml of CNF (n=6).

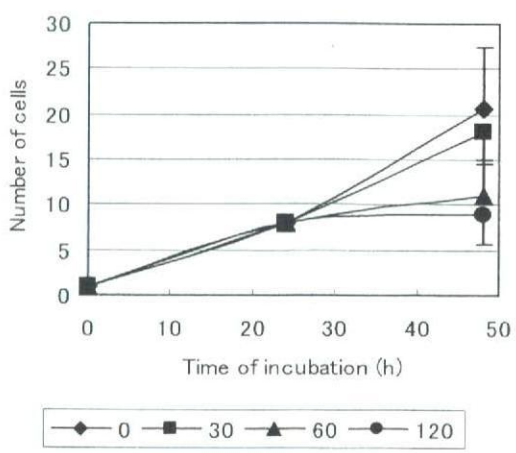

Fig. 3b. The time course of proliferation in different concentrations of CNF. The mean numbers of cells in fresh culture medium containing nutritive bacteria are shown (n=6). Diamond, 0; square, 30; triangle, 60; and circle, 120 µg/ml CNF. The abscissa shows time after the initiation of incubation and the ordinate the mean number of living

lower amount of CNF suspension. A single cell was suspended in 200 μl of culture medium containing bacteria in a glass depression slide culture. The time course of the CNF effect is shown in Fig. 3b. During the first 24 hours in bacteria-containing culture medium, CNF did not inhibit proliferation at any concentration. However, during the second 24 hours incubation, 60 and 120 μg/ml of CNF inhibited cell division.

The dose effect of CNF on proliferation at 48 hours after incubation is shown in Fig. 4. The mean number of cells at 30 μg/ml of CNF was about 80% of that of the control culture (Dunnett, $P<0.05$). At 60 μg/ml of CNF, the mean number of cells decreased to about 40% of the control (Dunnett, $P<0.01$), and remained at this level as the concentration of CNF increased. Thus, no dose effect was observed above 60 μg/ml of CNF.

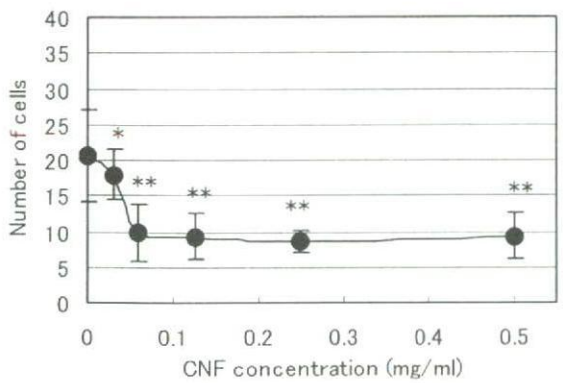

Fig. 4. Dose effect of CNF on proliferation. The abscissa shows the concentration of CNF and the ordinate the mean number of surviving cells at 48 h after the initiation of incubation. Bars show the standard deviation and * indicates a significant statistical difference at $P<0.05$ (Dunnett test) and * * at $P<0.01$ (Dunnett test) (n=6).

Reversibility of the cytotoxicity effect of CNF

The reversibility of cytotoxicity of CNF was examined by transferring paramecia cultured for 48 hours in various CNF concentrations to CNF-free fresh culture medium in a glass depression slide. As shown in Fig. 5, at 30, 60 and 125 μg/ml of CNF, the mean number of cells at 48 hours incubation recovered to control levels (CNF: 0 μg/ml). At 250 and 500 μg/ml, the mean number of cells did not recover fully, although statistical analysis showed no significant differences among the CNF concentrations (Dunnett, $P<0.09$ at 250 μg/ml).

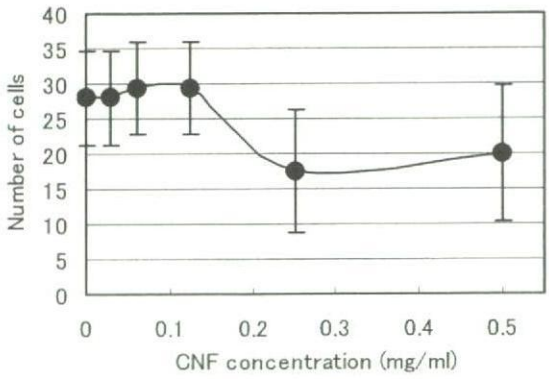

Fig. 5. Recovery of proliferative activity after removal of CNF. The abscissa shows the concentration of CNF and the ordinate the mean number of surviving cells at 48 h after the initiation of incubation. Bars indicate standard deviations (n=6).

DISCUSSION

The health risks to humans and other organisms from exposure to nanoparticles in the environment are one of the most important concerns regarding the use of these potentially valuable materials. The *Paramecium* bioassay system described here provides a useful means by which to determine the cytotoxicity of environmental and ingested CNF.

Paramecia play an important role in food webs in aquatic ecosystems. They ingest diverse bacteria growing in water (Taylor, 1979) and, in turn, are

eaten by other protozoa such as amoebas, didinia and other metazoan animals or their larvae (Porter et al, 1979; Taylor, 1980). Thus, CNF could move into food webs of aquatic ecosystems following ingestion by paramecia. The speed of a CNF-containing food vacuole formation and the maximum number in a cell were similar to those observed after ingestion of nutritive bacteria (data not shown)

Two types of nuclear division occur in *Paramecium*: mitotic nuclear division performed by the micronucleus, and amitotic division by the macronucleus. For the purposes of this article, the cells incubated in K-DS are referred to as "non-proliferating" cells.

At the beginning of this study, we set two categories of cellular properties for an assessment of the cytotoxicity effect of CNF. One is the property of cell survival and the other cell division. For cell survival tests we used the buffered saline, K-DS, and examined survival ratio and swimming behavior. In non-proliferating paramecia, CNF had no cytotoxicity effect on both cellular properties in all experiments performed in this study.

However, we have found strong cytotoxic effect of CNF in the cell division tests. In this test we used culture medium containing lettuce juice and nutritive bacteria as described in "Materials and Methods". The cytotoxic effect of CNF was observed in both properties of cell survival and cell division. At 50 mg/ml of CNF, cytotoxic effect was detected in the property of cell division during the initial 24-hour incubation and no effect on the property of cell survival. In the following 24-hour incubation, however, cytotoxic effect was detected in the property of cell survival, too.

We considered the possibility of causal relation of CNF effect on the property of cell survival. The simplest case is the inhibition of energy source uptake by CNF. But, it is hard to assume this case because, under our experimental conditions, paramecia can survive more than 1 week without any nutrient biomaterials indicating that the energy pool of cytoplasm is enough for surviving in the period of experiments performed in this study. However, an energy source uptake under the presence of CNF is remained to estimate experimentally.

An alternative possibility is the production of hazardous chemical substances by interaction between the metabolic products of culture medium and CNF. At this moment we have no information about chemical compositions of the culture medium. However, one candidate of the hazardous chemical substances is suggested by the following observation. One of the remarkable characteristics observed regarding cytotoxicity of CNF was the cessation of ciliary movement on the cell surface of proliferating paramecia. Ciliary movement in paramecia is essentially controlled by membrane potential (Dunlap, 1977; Kung and Saimi, 1982). Because the control of membrane potential is dependent on several kinds of ion channels (Kung and Saimi, 1982), chemical substances that affect ion channel functions will be one of target molecules to understand cytotoxicity of CNF.

Alternative experimental approach to the molecular mechanisms of CNF cytotoxicity is the use of complete synthetic culture medium in a cell division test. In this experiment we could systematically change chemical compositions in culture medium, so that the cytotoxicity of CNF control.

As shown in Fig. 4, the dose effect of CNF cytotoxicity was biphasic: at lower concentrations (from 30 to 60 μg/ml of CNF), a dose dependency was observed, while the effect appeared independent of dose at higher concentrations (from 60 to 500 μg/ml of CNF). The number of cells in culture medium depends on both the number of cell divisions and the number of cell death during cultivation. To obtain precise information about the contribution of cell division and cell death we have to perform a single cell isolation line culture under the presence of CNF after every cell division in

future experiments.

Our findings indicate that the effect of CNF on living organisms might not be as simple as previously predicted. We anticipate the presence of some complexity involving the molecular interactions between CNF and intracellular chemicals, which, in turn, may have harmful effects on cells.

In summary, the *Paramecium* bioassay system reveals that it is important to distinguish the property of cell division and cell survival in the elucidation of CNF cytotoxicity. As our studies have indicated, developing the appropriate regulatory guidelines to ensure the safety of nanotechnology will require biochemical examination and identification of chemical substances that interact with and modulate CNF cytotoxicity.

ACKNOWLEDGMENTS

Research was performed under Health and Labor Sciences Research Grants for Research on Risk Assessment of Chemical Substances: "Development of Visualization Method of Dynamical Motion Behavior of Nanoparticles in the Internal Body (H18-Chem-General-006)" from Ministry of Health, Labor and Welfare of Japan.

REFERENCES

Brown, D. M., Wilson M. R., MacNee W., Stone V., and Donalodson K. (2001) Size-dependent proinflammatory effects of ultrafine polystyrene particles: A role for surface area and oxidative stress in the enhanced activity of ultrafines. Toxicology and Applied Pharmacology 175, 191-199.

Dunlap, K. (1977) Localization of calucium channels in *Paramecium caudatum*. J. Physiol. 271, 119-133.

Dryl, S. (1959) Antigenic transformation in *Paramecium aurelia* after homologous antiserum treatment during autogamy and conjugation. J. Protozool., 6 (Suppl.), 25.

Haga, N. and Hiwatashi, K. (1981) A protein called immaturin controlling sexual immaturity in *Paramecium*. Nature 289, 177-179.

Hiwatashi, K. (1968) Determination and inheritance of mating type in *Paramecium caudatum*. Genetics 58, 373-386.

Iijima, S. (1991) Helical microtubules of graphitic carbon. Nature 354, 56-58.

Kung, C. and Saimi, Y. (1982) The physiological basis of taxis in *Paramecium*. Ann. Rev. Physiol. 44, 519-534.

Porter, K.G., Pace, M.L. and Batte, J. F. (1979) Ciliate protozoans as links in fresh-water planktonic food chains. Nature 277, 563-565.

Rajimi, P. S., Krishnakumari, M. K., and Majumder, S. K. (1989) Cytotoxicity of certain organic solvents and organophosphorus insecticides to the ciliated protozoan *Paramecium caudatum*. Microbios 59, 157-163.

Rodriguez, N.M. (1993) A review of catalytically grown carbon nanofibers. J. Matter Res., 8, 3233-3250.

Smith-Sonneborn, J., Palizzi, R.A., McCann, E.A., and Fisher, G.L. (1983) Bioassay of genotoxic effects of environmental particles in a feeding ciliate. Environ Health Perspect. Sep; 51, 205-210.

Smith-Sonneborn, J., Leibovitz, B., Donathan, R., and Fisher, G.L. (1986) Bioassay of environmental nickel dusts in a particle feeding ciliate. Environ. Mutagen. 8 (4), 621-626.

Taylor, W.D. (1979) Overlap among cohabiting ciliates in their growth responses to various prey bacteria Can. J. Zool., 57, 949-951.

Taylor, W.D. (1980) Observation on the feeding and growth of the predacious oligochaete *Chaetogaster langi* on ciliated protozoa. Trans. Am. Microsc. Soc., 99, 360-367.

Tohji, K., Goto, T., Takahashi, H., Shinoda, Y.,

Shimizu, N., Jeyadevan, B., Matsuoka, I., Saito, Y., Kasuya, A., Ohsuna, T., Hiraga, K., and Nishina, Y. (1996) Purifying single-walled nanotubes. Nature 383, 679.

Yanagi, A. (1987) Positional control of the fates of nuclei produced after meiosis in *Paramecium caudatum*: analysis by nuclear transplantation. Dev. Biol. 122, 535-539.

Available online at www.sciencedirect.com
SCIENCE DIRECT®
Materials Science and Engineering C 26 (2006) 675 – 678
MATERIALS SCIENCE & ENGINEERING C
www.elsevier.com/locate/msec

Apatite formation on carbon nanotubes

Tsukasa Akasaka [a,*], Fumio Watari [a], Yoshinori Sato [b], Kazuyuki Tohji [b]

[a] *Department of Biomedical, Dental Materials and Engineering, Graduate School of Dental Medicine, Hokkaido University, Sapporo, 060-8586, Japan*
[b] *Graduate School of Environmental Studies, Tohoku University, Sendai, 980-8579, Japan*

Received 1 November 2004; received in revised form 28 February 2005; accepted 28 March 2005
Available online 29 November 2005

Abstract

Apatite coating on carbon nanotubes (CNTs) was done with a biomimetic coating method. The multi-walled CNTs (MWNTs) of curled shape with about 30 nm in diameter were immersed for 2 weeks in the simulated body fluid. Observation by scanning electron microscopy (SEM) showed the formation of apatite on the MWNTs surface. The clusters of spherules consisting of needle-shaped apatite crystallites were massively grown on the aggregated MWNTs. The crystallites of 100 nm in width and 200–500 nm in length were grown perpendicularly to the longitudinal direction and radially originating from a common center of a single MWNT. Thus, the architecture of crystalline apatite at nano-scale levels could be produced by simple method and the MWNT may be acting as core for initial crystallization of apatite.

Keywords: Carbon nanotubes; Biomimetic coating; Apatite

1. Introduction

Carbon nanotubes (CNTs) have been attracting considerable attention because of their unique physical properties and potential for a variety of applications. The modifications of CNTs have been extensively investigated because of their relevance in electrical, mechanical and biological applications [1–8]. Immobilization of various functional molecules on CNT has also been examined in past studies [9–12]. For biomedical applications, new modification methods to give biocompatibility are needed for achievement of various required designs [13,14].

Biomineralization is a natural process in human being and animals, resulting in the formation of bones and teeth. Ca–P solution, such as the simulated body fluid (SBF), has been frequently used for the biomimetic Ca–P coating to increase the bioactivity, and has been successfully applied to implant materials for some special dental and medical cases [15–17].

Here we developed a biomineralization method to produce the architecture of apatite crystallites at nano-scale levels on the surface of MWNTs.

2. Experiment

The MWNTs used in this study were obtained from NanoLab (Brighton, MA, USA). The MWNTs of curled shape with about 30 nm in diameter were produced by the chemical vapor deposition (CVD) method. The raw MWNTs were refluxed in 6 N HCl solution and then washed thoroughly with deionized water and completely dried. Typical SEM (HITACHI S-4000) images of purified MWNTs are shown in Fig. 1.

The MWNTs material was dispersed in calcium phosphate solutions at a concentration of 10 mg/l by ultrasonication for 10 min. Then, the apatite crystallites were grown by immersing the MWNTs at 37 °C for various periods up to 2 weeks. The composition of the calcium phosphate solutions is as follows.

Revised SBF (R-SBF): NaCl (866 mg/l), $CaCl_2$ (125 mg/l), K_2HPO_4 (803 mg/l), KH_2PO_4 (326 mg/l), KCl (625 mg/l), $MgCl_2$ (59 mg/l) containing NaF (22 mg/l) and the pH was adjusted to 7.2 using KOH and no precipitation was observed in the solution during the experimental period.
Dulbecco's phosphate-buffered saline (PBS(+)): NaCl (8000 mg/l), $CaCl_2$ (100 mg/l), KH_2PO_4 (200 mg/l), Na_2HPO_4 (1150 mg/l), KCl (200 mg/l), $MgCl_2$ (47 mg/l) containing NaF (22 mg/l) and the pH was adjusted to 7.4 using KOH

* Corresponding author. Tel.: +81 11 706 4251; fax: +81 11 706 4251.
E-mail address: akasaka@den.hokudai.ac.jp (T. Akasaka).

0928-4931/$ - see front matter © 2005 Elsevier B.V. All rights reserved.
doi:10.1016/j.msec.2005.03.009

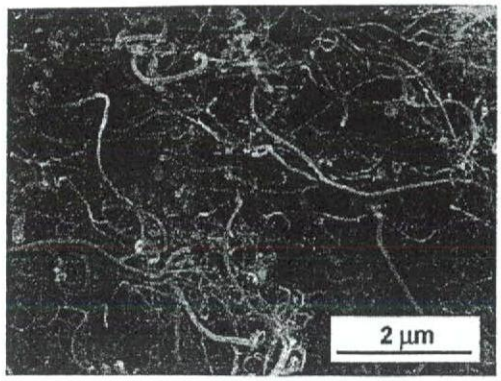

Fig. 1. SEM images of purified MWNTs.

and no precipitation was observed in the solution during the experimental period.

Standard SBF (S-SBF): NaCl (7996 mg/l), $CaCl_2$ (278 mg/l), K_2HPO_4 (174 mg/l), KCl (244 mg/l), $NaHCO_3$ (350 mg/l), $MgCl_2$ (143 mg/l), Na_2SO_4 (71 mg/l), $(CH_2OH)_3CNH_2$ (6057 mg/l), 1 M HCl (40 ml) containing NaF (22 mg/l) and the pH was adjusted to 7.4 using KOH.

Finally, the resultant MWNTs were separated from the suspension by filtration, gently washed with deionized water to remove impurities, and then dried at 60 °C for 6 h. In order to study the effects of immersing time-course on apatite growth, they were immersed for 6 h, 1 day, 2 days, and 2 weeks. To compare the influence of the substrates, we also use a square piece of carbon plate ($10 \times 10 \times 1$ mm^3) (Nirako, Japan) instead of MWNTs.

The formation of apatite on the MWNTs surface was investigated by SEM after coating with carbon. Transmission infrared spectra were performed by the KBr method using a fourier transmission infrared spectrometer (FT-IR, JASCO FT/IR-300E) in the wave number region 400–4000 cm^{-1} collected at resolutions of 4 cm^{-1}. Commercial hydroxyapatite (Seikagaku Corp.) was used as a control.

3. Results and discussion

3.1. Apatite formation in R-SBF

Zhao and Gao recently reported that hydroxyapatite nanoparticles decorated on the sodium dodecyl sulfate (SDS) adsorbed MWNTs by an in situ synthetic method with calcium nitrate, $Ca(NO_3)_2$, and ammonium secondary phosphate, $(NH_4)_2HPO_4$ [18]. In contrast, our strategy for the apatite formation consists of biomimetic coating on the surface of MWNTs in the calcium phosphate solutions such as a SBF.

To optimize this strategy, we first studied the apatite formation on MWNTs in R-SBF. After immersion for 2 weeks, the MWNTs apparently became the gray in the solution. SEM images show the massive growth of the clusters of apatite crystallites with a needle-like shape on the aggregated MWNTs (Fig. 2A). Acicularly grown crystallites with about 150 nm in diameter form the bloom-shape morphology. A further detailed observation clearly showed that the crystallites of 100 nm in

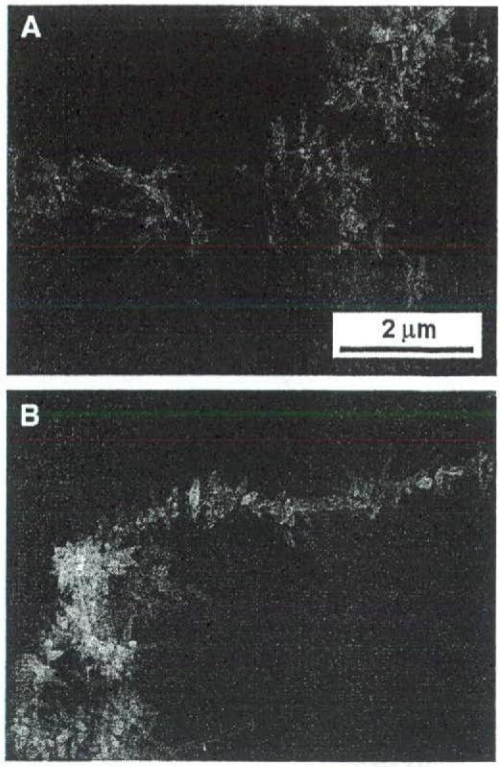

Fig. 2. SEM images of apatites: (A) needle crystallites grown radially on MWNT core; (B) barbed wire shape of crystallites on a MWNT core.

width and 200–500 nm in length were grown radially originating from a common center in the middle of a single MWNT and perpendicularly to the longitudinal direction of MWNT. In part, there exist bowknot-like bundles with their two ends fanning out while the middle part tying together [19]. Barbed wire-like-shaped feature in Fig. 2B was also observed.

From these results, the needle-like apatite crystallites were directly grown starting from the surface of MWNT. Thus, the MWNT may be acting as core for initial crystallization of the apatites. However, in this condition, the reproducibility of sizes and shapes of apatites formed on MWNTs was poor because R-SBF was highly supersaturated and was difficult to handle.

Fig. 3 shows the infrared transmission spectra of the apatite/MWNTs after immersion in R-SBF for 2 weeks. Compared with the spectrum of commercial hydroxyapatite as a control, very similar peaks at around 3440, 1099, 1040, 966, 607 and 569 cm^{-1} on the spectrum were observed. The bands at 3440

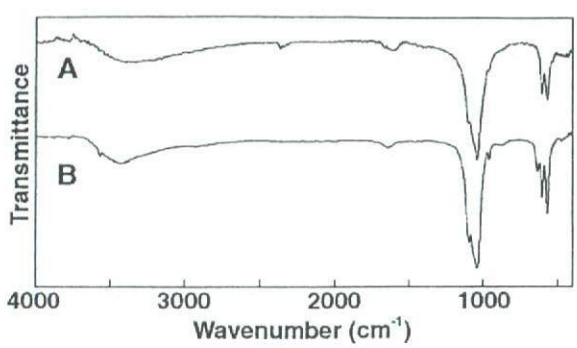

Fig. 3. FT-IR spectra of the apatite/MWNTs after immersion in R-SBF for 2 weeks (A) and hydroxyapatite as a control (B).

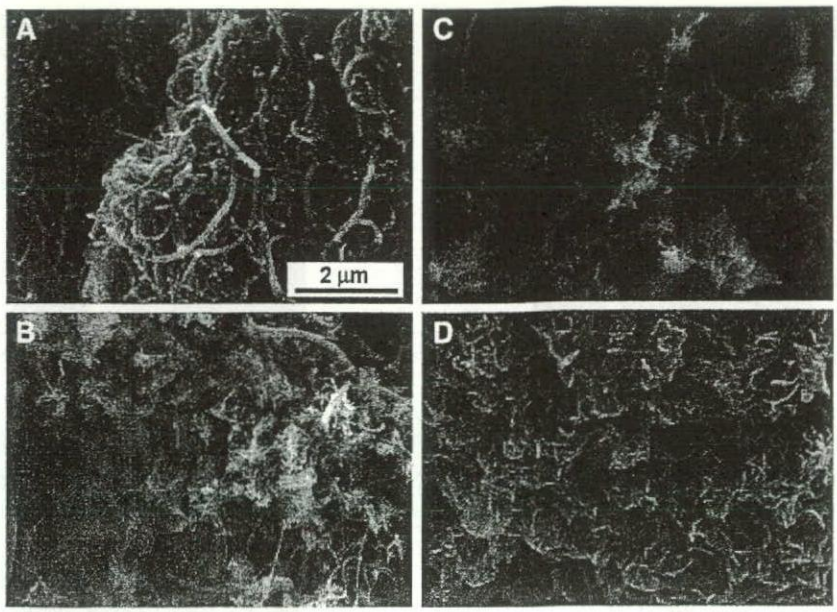

Fig. 4. SEM images of the apatite/MWNTs in PBS(+) after immersion for 6 h (A), 1 day (B), 2 days (C), and 2 weeks (D).

cm^{-1} and 1640 cm^{-1} may come from lattice H_2O. The phosphate modes 1046 cm^{-1} ($\nu_3(PO_4)$), 1029 cm^{-1} ($\nu_3(PO_4)$), 959 cm^{-1} ($\nu_1(PO_4)$), 590 cm^{-1} ($\nu_4(PO_4)$), and 577 cm^{-1} ($\nu_4(PO_4)$) are observed. However, no peaks were observed at 3536 and 633 cm^{-1}, which exist in the commercial hydroxyapatite and assigned to −OH stretch and −OH liberation, respectively. The spectrum of hydroxyapatite clearly shows the bands corresponding to hydroxyl groups. The spectrum of the apatite/MWNTs formed in R-SBF was similar to that reported by Harrison et al. [20] and may be composed of partly fluorided apatite [21,22].

3.2. Influence of the time-course and substrate changes in PBS(+)

Fig. 4 presents the SEM images of the apatite/MWNTs after immersion in PBS(+). With the increase of immersion time (1 day to 2 weeks), the size of apatite crystallites increased. The growth on the MWNTs started with a nano-sized flake-like crystallite on 1 day (Fig. 4B) and followed by a constant growth during 2 weeks. The morphology was changed to the thicker leaf flake-like shape. After 2 weeks, the apatite crystallites showed the complete coverage over the aggregate of MWNTs (Fig. 4D). There was some incubating time for apatite nucleation. SEM did not observe apatite formation on surface up to 6 h immersion on the MWNTs treated with PBS(+) (Fig. 4A). Once the apatite nuclei are formed, they can grow spontaneously by consuming calcium and phosphate ions from PBS(+), since PBS(+) is already highly supersaturated with respect to apatite.

On the other hand, the immersion of MWNTs in S-SBF showed no apatite formation after 2 weeks (data not shown here). The S-SBF was stable without the precipitation during immersion for up to 2 weeks, while both R-SBF and PBS(+) were unstable. For nucleation to occur, an activation energy barrier must be exceeded. This activation energy can be decreased by increasing the degree of supersaturation of calcium phosphate solutions. Thus, in the strategic point of view to modify MWNTs surface, it is effective to immerse in the higher supersaturated solutions as R-SBF or PBS(+).

The apatite formation in PBS(+) after a 2-week immersion was compared using SEM on both carbon plate and MWNTs substrates. Carbon plate substrate showed much less apatite formation sites than MWNTs. The few apatites formed on the carbon plate near its edge have a similar morphology as those formed on the MWNTs surface (Fig. 5). The results indicated

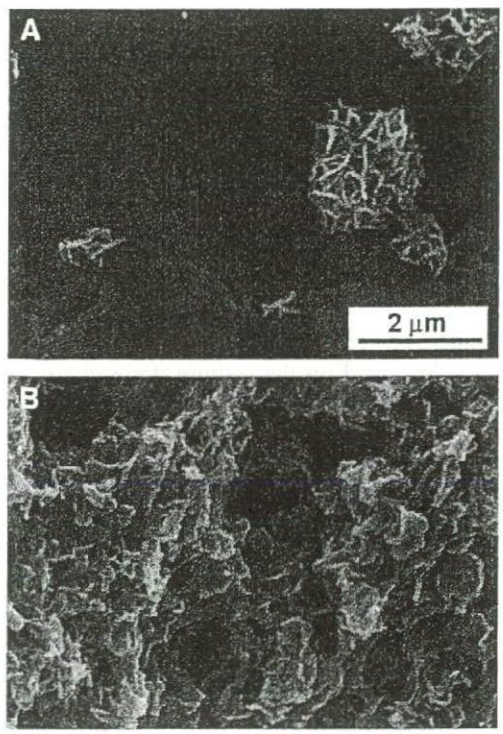

Fig. 5. SEM images of the apatites precipitated on carbon plate (A) and MWNTs in PBS(+) after 2 weeks (B).

that MWNTs have the stronger affinity for nucleation than carbon plate.

4. Conclusions

A simple route was developed to synthesize the apatite/MWNTs using the higher supersaturated calcium phosphate solution at ambient conditions. We obtained the apatites on the MWNT surface with different size and morphology within 2 weeks. The nano-sized apatite crystallites were produced in R-SBF for 2 weeks with a width of about 100–200 nm and a length of about 200–500 nm. The comparison of the apatite formation on both carbon plate and MWNTs substrates revealed significant differences in the density of apatite crystallites. The MWNT substrate showed much apatite formation more favorable than carbon plate. The results indicated that the MWNT acts as an effective nucleation surface to induce the formation of a biomimetic apatite coating. MWNTs with the defined surface morphology of nano apatite crystallites could be useful as biomaterials for scaffolds and for the biomedical applications.

Acknowledgements

This study was supported by Grant-in-Aid for Research on Nano-Medicine H14-nano-021 from Ministry of Health, Labor and Welfare of Japan.

References

[1] A. Hirsch, Angew. Chem., Int. Ed. Engl. 41 (2002) 1853.
[2] J.L. Bahr, J.M. Tour, J. Mater. Chem. 12 (2002) 1952.
[3] Y.P. Sun, K. Fu, Y. Lin, W. Huang, Accounts Chem. Res. 35 (2002) 1096.
[4] B. Fugetsu, S. Satoh, T. Shiba, T. Mizutani, Y. Nodasaka, K. Yamazaki, K. Shimizu, M. Shindoh, K. Shibata, N. Nishi, Y. Sato, K. Tohji, F. Watari, Bull. Chem. Soc. Jpn. 77 (2004) 1945.
[5] B. Fugetsu, S. Satoh, A. Iles, K. Tanaka, N. Nishi, F. Watari, Analyst 129 (2004) 565.
[6] K. Tamura, N. Takashi, T. Akasaka, I.D. Rosca, M. Uo, Y. Totsuka, F. Watari, Bioceramics 16 (2004) 919.
[7] K. Tamura, N. Takashi, R. Kumazawa, F. Watari, Y. Totsuka, Mater. Trans. 43 (2002) 3052.
[8] A. Yokoyama, Y. Sato, Y. Nodasaka, S. Yamamoto, T. Kawasaki, M. Shindoh, T. Kohgo, T. Akasaka, M. Uo, F. Watari, K. Tohji, Nano Lett. 5 (2005) 157.
[9] S.C. Tsang, Z. Guo, Y.K. Chen, M.L.H. Green, H.A.O. Hill, T.W. Hambley, P.J. Sadler, Angew. Chem., Int. Ed. Engl. 36 (1997) 2198.
[10] C.V. Nguyen, L. Delzeit, A.M. Cassell, J. Li, J. Han, M. Meyyappan, Nano Lett. 2 (2002) 1079.
[11] W. Huang, S. Taylor, K. Fu, Y. Lin, D. Zhang, T.W. Hanks, A.M. Rao, Y.P. Sun, Nano Lett. 2 (2002) 311.
[12] M. Shin, N.W.S. Kam, R.J. Chen, Y. Li, H. Dai, Nano Lett. 2 (2002) 285.
[13] T. Akasaka, K. Matsuura, N. Emi, K. Kobayashi, Biochem. Biophys. Res. Commun. 260 (1999) 323.
[14] T. Akasaka, K. Matsuura, K. Kobayashi, Bioconjug. Chem. 12 (2001) 776.
[15] H.-M. Kim, T. Miyazaki, T. Kokubo, T. Nakamura, Key Eng. Mater. 192–195 (2001) 47.
[16] A. Oyane, M. Kawashita, K. Nakanishi, T. Kokubo, M. Minoda, T. Miyamoto, T. Nakamura, Biomaterials 24 (2003) 1729.
[17] W.-W. Song, Y.-K. Jun, Y. Han, S.-H. Hong, Biomaterials 25 (2004) 3341.
[18] L. Zhao, L. Gao, Carbon 42 (2004) 423.
[19] J. Liu, K. Li, H. Wang, M. Zhu, H. Yan, Chem. Phys. Lett. 396 (2004) 429.
[20] J. Harrison, A.J. Melville, J.S. Forsythe, B.C. Muddle, A.O. Trounson, K.A. Gross, R. Mollard, Biomaterials 25 (2004) 4977.
[21] Q. Williams, E. Knittle, J. Phys. Chem. Solids 57 (1996) 417.
[22] L.M. Rodriguez-Lorenzo, J.N. Hart, K.A. Gross, Biomaterials 24 (2003) 3777.